Future Cities and Environment

Xu, W, et al. 2021. A Coupled Modelling Method for the Evaluation of the Impact of Pavement Solar Collector on Urban Air Temperature and Thermal Collection. *Future Cities and Environment,* 7(1): 2, 1–16. DOI: https://doi.org/10.5334/fce.109

TECHNICAL ARTICLE

A Coupled Modelling Method for the Evaluation of the Impact of Pavement Solar Collector on Urban Air Temperature and Thermal Collection

Weijie Xu, Carlos Jimenez-Bescos, Conrad Allan Jay Pantua, John Calautit and Yupeng Wu

The Urban Heat Island (UHI) effect is a phenomenon whereby urban areas become warmer than their surrounding rural areas, due to the replacement of vegetation and soil with surfaces such as asphalt and concrete. The asphalt pavement surfaces tend to absorb a large amount of heat through solar radiation and increase the air temperature, which affects the operation of building heating and cooling systems, causing environmental problems and thermal discomfort. However, this energy can be collected by water circulated through buried copper pipes to cool down temperatures and be stored for other usages. This work aims to develop a method for determining the optimum areas to locate pavement solar collector (PSC) systems and simulate the reduction of ambient air and surface temperature by using a coupled computational modelling approach. Discrete ordinate model and solar-ray tracing were utilised for solar radiation effect modelling in the 3D simulation. Furthermore, the PSC prototype was developed, and lab-scale experiments were carried out for validation. Based on the simulated conditions, in the unshaded area, the asphalt slab's near-surface temperature was reduced by up to 10℃ and the outlet water temperature increased by about 5℃. At the pedestrian height level, the air temperature was reduced up to 4.6℃. This study further expands the investigation of the variation of outdoor conditions such as air temperature and solar radiation. The results showed that the proposed method could be used to optimise the pavement solar collector's positioning to reduce urban surface and air temperature.

Keywords: Pavement solar collector; Computation Fluid Dynamics (CFD); urban street canyon; Urban Heat Island (UHI); thermal collection; heat mitigation

1. Introduction

Urban heat island (UHI) phenomenon is caused by urban overheating, which is becoming a severe problem for many major cities in the world (Santamouris, 2020). The solar energy absorbed by artificial surfaces such as building and ground surfaces, then the heat is emitted from the surfaces to the urban environment. The microclimate of urban areas is more complex and usually has higher temperatures than rural areas due to the UHI phenomenon. The increased ambient temperature may cause thermal discomfort; high discomfort can lead to high energy and cost utilisation, further worsening the issue (Lin et al., 2020). The quality of the building's thermal environment is dependent on the urban settings and local climate. Building energy consumption could be significantly impacted by the UHI effect by increasing the energy required for space cooling (Sun and Augenbroe, 2014, Ciobanu et al., 2014). The study (Santamouris et al., 2015) concluded that the peak electricity load could increase between 0.45% and 4.6% for each degree C of temperature increase. A case study in Rome, Italy showed that the building cooling energy demand increased by 30% because of the UHI phenomenon, and the heating energy demand decreased by 11% (Guattari et al., 2018). When there are low winds and the sky is clear, the UHI phenomena would be intensified. While, high wind velocity could increase the atmospheric flowing, which reduces the temperature difference between urban and rural areas.

It is highlighted by Evola et al. (2017) that the pavement is one of the essential urban features that influence the microclimate and building energy performance. Conventional pavement or asphalt pavements can absorb a large amount of light and radiation, and the heat is dissipated to the surrounding air, which further aggravates the UHI effect. It is found that the pavement temperature could be much higher than the ambient air temperature (Berdahl and Bretz, 1997). Although the reflection and

Department of Architecture and Built Environment, University of Nottingham, UK

Corresponding author: Weijie Xu (weijie.xu@nottingham.ac.uk)

absorption of radiative heat of pavement can affect the air temperature, both short-wave radiation and long-wave radiation impact the pedestrians' thermal comfort. Short-wave radiation refers to the sunlight, which comes from the sun surface with extremely high temperature, long-wave radiation is emitted by the atmosphere and terrestrial surfaces including buildings and ground, the temperatures are relatively low (Ma et al., 2019). Pavements are taking up a large proportion of urban areas, which could highly contribute to the development of UHI (Santamouris, 2013). High road surface temperature can cause high air temperature, which not only leads to the uncomfortable thermal environment for pedestrians; it could also shorten the car tyres' life span (DKT, 2020). As it covers a significant percentage of the urban surface, urban pavements are significant contributors to the increasing in urban temperature, which attracts numerous multidisciplinary researches concerning urban heating and development of solutions to mitigate the heat island effects such as the use of vegetation, solar collectors and cool/reflective pavements. Using appropriate solar controls and shadings for urban surfaces can also reduce the impact of UHI (H. Akbari, 2001) – studies by (Sailor, 1995, Gaitani et al., 2007) shown that pavement surfaces take an essential part of the overall urban thermal balance. Compared to other mitigation methods such as green roofs, parks and cool roofs, the study showed that "cool pavements" could provide a higher reduction in air temperature.

Santamouris (2013) concluded that cool pavements showed high mitigation and cooling potential, reducing the sensible heat flux to the atmosphere and then decreasing the temperature on the urban environment significantly. Previous studies have introduced several methods to improve the thermal performance of pavements: (a). increase pavement surface albedo to reduce the absorption of solar radiation (reflective pavements) (Mallick, 2009), (b). increase the pavements' permeability to decrease the surface temperature by evaporation (Karasawa et al., 2006), (c). add high thermal materials or capacitance of latent heat storage to increase pavement surfaces' thermal storage capacity (Santamouris, 2013), (d). use natural or artificial solar control devices to provide shadings for pavement areas (Santamouris, 2013) and (e). install external mechanical systems to reduce pavement surface temperature, including circulation of water or other fluid in the pavement mass to remove excess heat (Mallick, 2011, Mallick, 2009), simulations and experiments showed the system's thermal potential is quite high.

Pavement solar collector (PSC) is a system that allows heat to be transferred from the surface to the bottom layers, which is then absorbed by the water circulated through a series of pipes. Therefore, the working fluid could reduce the pavement surface temperature and at the same time, extract and utilise the heat energy. PSC showed higher potential to mitigate overheating than other solutions (Evola et al., 2017). **Figure 1** illustrates the typical heat transfer between pavement and building; the asphalt pavement absorbs the solar radiation, the heat is stored in the pavement and then radiated to the air and building external walls, which heats the street air temperature and building surfaces. The heat can transfer into the building by convection, which increases the building's cooling load during the summer. The PSC system's water pipes can remove the heat from the pavement and cool down the pavement surface temperature. When the adjacent air temperature decreases, it can provide a better thermal environment for pedestrians in summer. The study by Papadimitriou et al. (2019) highlighted PSC's potential to provide the urban environment's thermal energy requirements. The thermal energy collected by the PSC system can be stored and then used for covering buildings' thermal loads, and other city facility needs (Chen et al., 2009, Wang et al., 2011), such as water heating for neighbouring buildings and snow melting (Daniels et al., 2019).

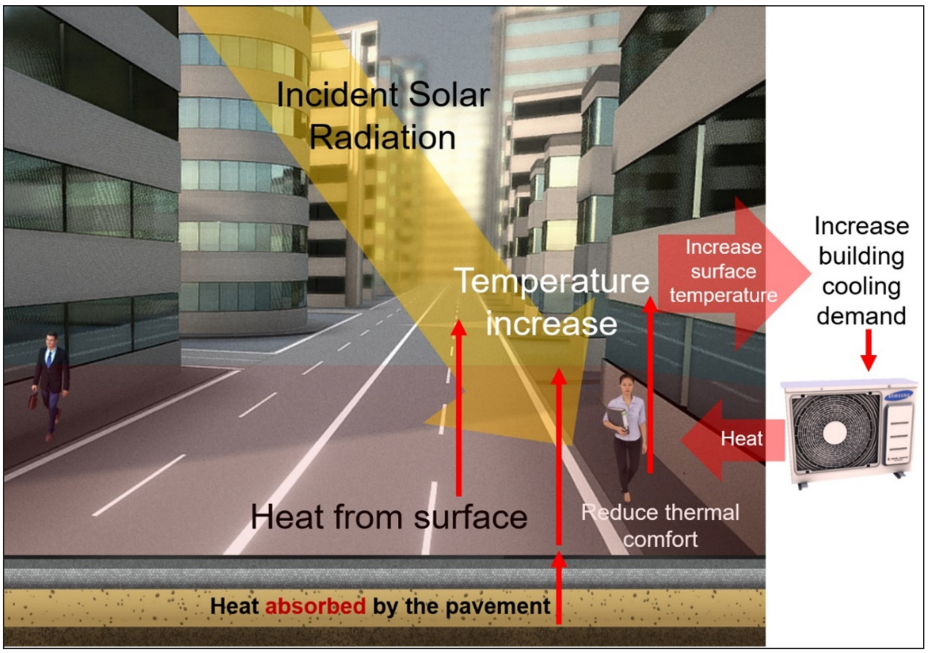

Figure 1: Typical heat transfer in an urban area with standard pavement, modified from (Sketchfab, 2020).

During the summer days, the system could reduce the extremely high surface temperature of the asphalt pavement and air temperature within urban environments (Hasebe, 2016). Due to the UHI effect, the PSC system's efficiency in urban is higher than in rural areas. The study by Chen et al. (2009) showed that the PSC system could reduce the surface temperature by up to 5°C, reducing the UHI effect and potentially extending the lifecycle of pavements up to 5 years. During the winter, the work (Daniels et al., 2019) proposed that the heated pavement systems can be used for snow melting and de-icing. The experiment showed that during winter daytime, when the sky is clear, the system could raise the storage temperature to 11.5°C and the pavement could maintain a snow-free surface under the condition of subfreezing with six hours snowfall.

Guldentops et al. (2016) developed a model of a solar pavement collector for extracting low-temperature thermal energy; the impact of ageing on system performance was also investigated. It was found that, when the colour of the asphalt concrete becomes lighter, more incident solar radiation will be reflected and therefore, the collector efficiency will drop to about 16% and the absorptivity will drop from 0.95 to 0.65. Chiarelli et al. (2017) evaluated the optimisation of convection-powered asphalt collectors to reduce urban pavement temperatures using experimental trials and CFD simulations. The study concluded that optimal performance was achieved when the PSC pipes were installed in a single row under the pavement, allowing for a surface temperature reduction of up to 5.5°C. According to Pascual-Munoz et al. (2013), the solar light irradiance, materials, flow rates of the heat transfer fluid (water) and collector geometry have an impact on the PSC system efficiency. Their work also found that the PSC system can decrease the ambient temperature and mitigate the UHI effect. Another work (Nasir et al., 2017a) has analysed the PSC system performance and assessed the influence of the pipe diameter, depth, inlet water velocity and inlet water temperature of PSC pipes. The asphalt pavements with higher conductivity tend to provide higher temperature, and solar energy would be transported faster (Guldentops et al., 2016). It is necessary to analyse how ageing affects pavement solar collector systems' performance, as the ageing process could have a negative impact on the thermal conductivity and absorptivity of the pavement surface.

The environmental parameters would also affect the performance of pavement solar collectors. The influence of building geometry, urban street canyon aspect ratio and urban form on the PSC system have been analysed in the previous works (Nasir et al., 2015, Nasir et al., 2017c, Nasir et al., 2017b). Memon et al. (2010) evaluated the role of wind speed and building aspect ratio (ranging between 0.5 and 8) on air temperatures in an urban canyon using CFD and comparing results with wind tunnel measurements; two diurnal and one nocturnal heating situation were considered. High building density would increase the urban temperature; however, the high-rise buildings could also provide shadings for the surrounding buildings and the pavements. Shading effects from the nearby buildings can reduce the UHI phenomenon. The surface temperature will be lower than those without shading, and the PSC system will collect less heat and hence must be considered during the initial stage. It is suggested by Yang et al. (2016) that pavements can have a significant impact on the wall temperature and building energy consumption in high-density residential area. The canyon geometry determined the performance of pavements in the urban canyon areas. Nasir et al. (2017c) showed that PSC's performance has significantly dropped (up to 30%) in shaded areas and the refraction of the solar radiation influences the temperature distribution on the ground. Considering economic benefits, it is necessary to analyse the PSC system's performance in a high-rise building area before putting into operation. It is mentioned by Papadimitriou et al. (2019) that by comparing the applications, features, and potentials among thermal collector pavements, electrical collector pavements and thermoelectric generator pavements, it shows that solar radiation intensity, ambient temperature, wind speed, pavement surface temperature, the layout of heat exchanger could also affect the performance of solar pavement systems.

1.1 Novelty and Gaps in Knowledge

Based on the review, previous studies focused on various methods for minimising the UHI phenomena. Numerous studies (Daniels et al., 2019, Bobes-Jesus et al., 2013) focused on the influential factors and parameters for improving the asphalt solar collectors heat collection efficiency. The work (Nasir et al., 2017a) investigated the influence of pipe layout, embedded pipe depth, pipe spacing, pipe diameter, the flow rate of the medium used for the heat transfer, thermal conductivity, etc. The impact of building geometry (Nasir et al., 2015) and street canyon aspect ratio (Nasir et al., 2017c, Nasir et al., 2017b) on the PSC system performance were also analysed using a decoupled approach. The decoupled approach simulates the urban canyon and PSC system separately and cannot predict the PSC's direct influence on the urban air temperature. In addition, it has limitations when it comes to transferring the temperature data from the urban canyon model to the PSC system model. The study (Guldentops et al., 2016) focused on model development and validation of the pavement solar collector system. However, no study evaluated the integration of urban street canyon and the PSC system in a computational domain or using a coupled approach for analysing the impact of the PSC systems on the surface-air temperature reduction and thermal collection. This is mainly due to the high requirements for computing power and resource to carry out such simulations which were not available previously. The building cooling energy demand will also decrease because of the lower air temperature. Therefore, to fully optimise the system, the heat transfer processes from the sun to the pavement, pavement to air and air to the building must be taken into account. It is envisaged that the proposed approach will also help the development of future models to assess the influence of the PSC on the energy demand of the neighbouring buildings i.e. in terms of affecting the local air temperature and providing heat to the build-

ings. It is necessary to combine the canyon, pavement and PSC system to simulate the temperature reductions and thermal collection at the same time. This has not been explored in previous research (Daniels et al., 2019, Bobes-Jesus et al., 2013, Nasir et al., 2017a) and the limitation of existing models. Little research discussed the influence of the urban environment on the thermal performance of pavement solar collectors. Furthermore, there is no research on the pavement solar collector system's influence and the urban environment conditions and vice versa.

1.2 Aim and Objectives

This work investigates the combined effect of the PSC system on building, air and road temperatures by modelling the heat transfer between the urban street canyon and pavement solar collectors using a coupled computational approach. A basic urban surface unit can be recognised as the urban canyon, the canyon includes walls and ground between two adjacent buildings, which can be used as the basic unit of urban areas in the built environment (M. Nunez and T. R. Oke, 1976). An array of pipes was embedded under the pavement located in the middle of an urban canyon to evaluate how the PSC system can affect the pavement surface temperature and surrounding air temperature. Computational Fluid Dynamics (CFD) simulation was used for this research which is widely used for analysing the aero-thermal environment of urban street canyons and pavement solar collectors (Ai and Mak, 2017). The weather data of Milan, Italy, was selected for this study and 20% of the road was embedded with the pipes. The study will compare the influence on the surface temperature and the ambient environment of pavement with and without the PSC system, also, assess the potential thermal collection. Six different water inlet velocities and temperatures were compared to show how it affects the PSC system's thermal performance. The asphalt slab prototype of PSC was built and tested in a laboratory setup to obtain the real-time temperature distribution across an asphalt pavement and validate the CFD modelling approach.

2. Method

The study developed a coupled approach to combine the urban street canyon domain and pavement with the same model's PSC system domain and simulate the heat transfer between the two solid-fluid domains. The coupled approach was used to: (i) observe the temperature distribution of the pavement, (ii) compare the air temperature of different positions of the street canyon, (iii) analyse the pipe outlet temperature and the amount of heat that can be dissipated.

For the present study, ANSYS FLUENT v18 was used to model the thermo-fluid properties of the system. FLUENT is a computational fluid dynamics software package used to model fluid dynamics, heat transfer and thermal reactions for diverse applications.

Figure 2 shows the methodology process. The geometry of both street canyon and pavement parts was generated in Solid Edge, and then the model was then imported to ANSYS for computational domain and mesh generation, boundary condition set up and simulation process. After generated the mesh, the mesh quality was checked to ensure it satisfied the simulation accuracy requirement. The CFD tool ANSYS Fluent with the standard turbulence k–ε model was used for the simulation and analysis. The CFD governing equations including continuity, momentum and energy are solved. The effects of solar radiation within the canyon are simulated using the discrete ordinates (DO) model. The SIMPLE algorithm solved the discretised equations was selected while the second-order central difference was utilised for spatial discretisation and in temporal discretisation. A workstation with a dual 32 core processor and 64GB RAM was used for conducting the simulations. The boundary conditions were set based on the material properties and local environment for a selected time and date of Milan, Italy (Nasir et al., 2017a, Nasir et al., 2017c). The input values included initial air temperature, pavement surface temperature, circulating water temperature and velocity. The simulated results were validated with experimental data. The output parameters from results included the pavement surface temperature and air temperature reduction due to the PSC

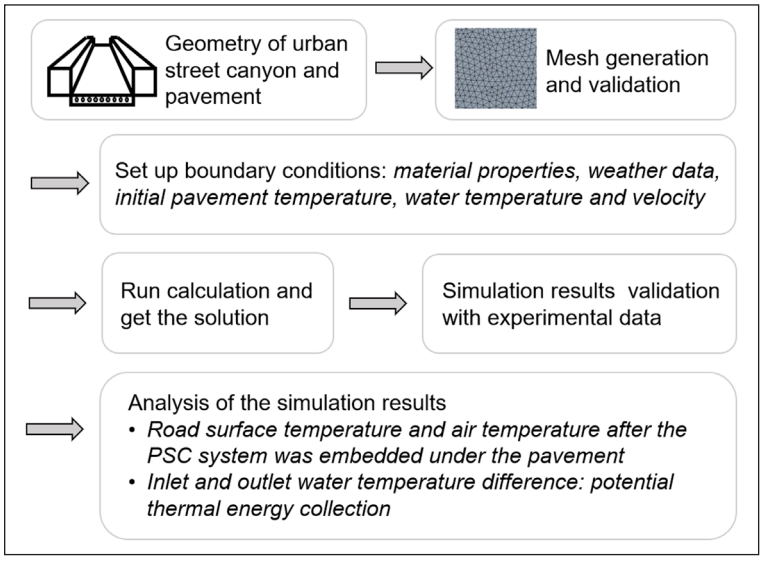

Figure 2: Methodological chart of the simulation process.

system. The inlet and outlet water temperature difference was used to show the potential thermal energy collection. ANSYS Fluent was also used for the post-processing and visualisation of results.

2.1 Geometry and computational domain

2.1.1 Urban domain

To understand the local atmospheric flow and other related processes, a street canyon can be used as the basic unit of urban areas in the built environment (Ai and Mak, 2017, Oke, 1987). The microclimate of the urban street canyon includes temperature, wind flow, pollutants, noise and other outdoor environmental parameters, which are associated with the indoor environmental quality of the nearby buildings (Ai and Mak, 2015). It is suggested by Zhu et al. (2007) and Bouyer et al. (2011) that the microclimate of street canyons influences the pedestrian thermal comfort and building energy performance.

According to Table 2.1 (Murphy, 2011), the principle road's width should be wider than 8.8 m, which includes the cycle lane. In the urban street canyon, the dimensions of the road between two buildings were 10.0 m with (W) and 100.0 m length (L). Building's height was 10.0 m (H), which the canyon aspect ratio (H/W) was 1. The urban street canyon domain is illustrated in **Figure 3**.

Side and top walls are set to symmetry walls, the distance between inflow and outflow were set to 5H, which was 50.0 m. The 3H height was selected for the distance between the ground and domain top lane to provide enough space for airflow circulating. The wind came from the inlet, which is perpendicular to the pavement direction (y-direction).

The whole domain was divided into two regions: (1). 0.3 m thickness solid pavement region and (2). air-fluid region (wind). This model's total macro domain was defined as 100.0 m length × 80.0 m width × 30.3 m height.

2.1.2 PSC domain

In order to find the temperature difference of road surface and air of the canyon, the pipes were not embedded for the whole pavement but only covered 20% of the pavement length. The pipes were made of copper, and the wall thickness was 0.009 m. The pipes were located in the centre of the pavement with a length of 20.0 m and a diameter of 0.02 m. The embedded depth was 0.15 m, and there were 9 pipes in the pavement, with an interval of 1.0 m (**Figure 3**). Therefore, this domain includes 9 copper pipes with a length of 20.0 m embedded within the solid pavement with 100.0 m length × 10.0 m width × 0.3 m depth.

2.2 Mesh and sensitivity analysis

Mesh size impacts the result accuracy; the smaller mesh can provide higher quality simulation results as there will be more nodes and elements of the object, which needs longer simulation time. However, the mesh size for the whole domain was not uniform in order to achieve faster computational times (Fluent, 2011).

The patch conforming method was applied to canyon sections, including building walls, building roofs and ground road surfaces. The mesh sizing for the PSC area was set to High, which can calculate a more accurate output value than Coarse and Medium. Mesh details are shown in **Table 1** and **Figure 4**.

2.3 Boundary conditions

Base on the previous studies (Nasir et al., 2015, Nasir et al., 2017b, Nasir et al., 2017c, Nasir et al., 2017a), in this research, the urban street canyon was located in Milan, Italy, for result validation, the latitude is 45.47°, and longitude is 9.18°. The selected time and date are 14:00 on 26th June, on that day the sunshine factor is 0.25. The wind came from the south direction with a temperature of 303K (29.85°C) and velocity of 2 m/s.

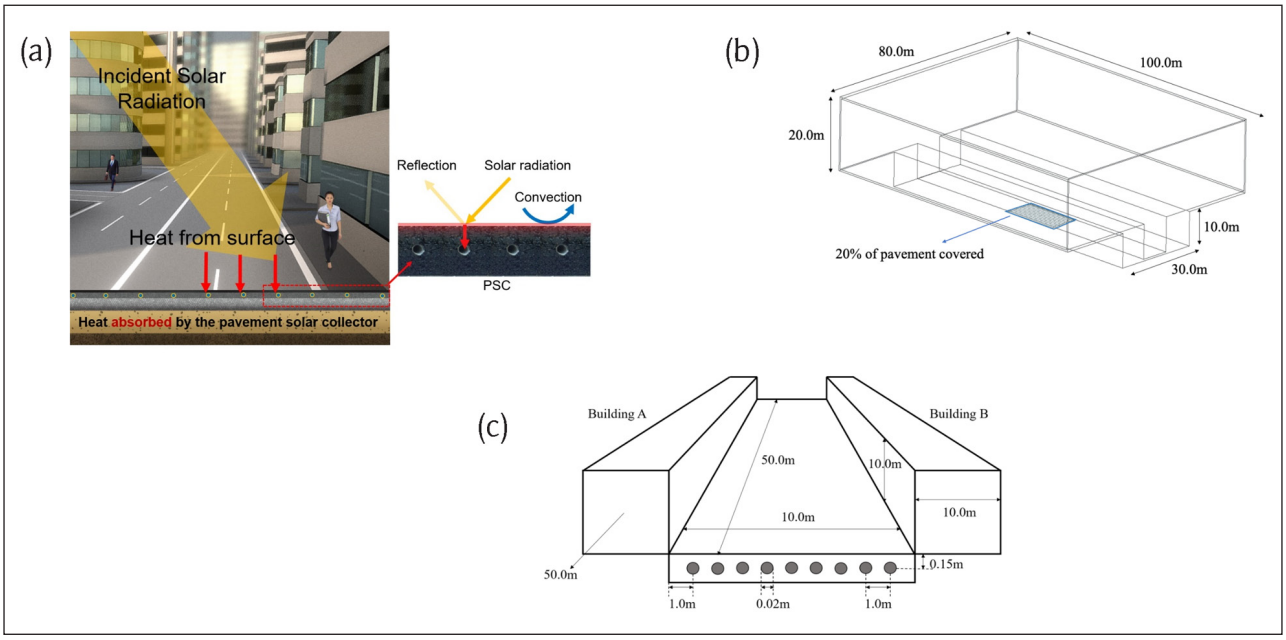

Figure 3: (a) Integration of PSC into an urban canyon **(b)** geometry of the whole domain and **(c)** location of the pipes (section from Figure 3 (a), not to scale).

Table 1: Mesh sizing.

Size	Mesh description	Total elements	Total nodes
Coarse	Patch conforming method	916,765	236,066
Medium	Patch conforming method	2,559,796	698,871
High	Patch conforming method	6,048,503	1,785,968

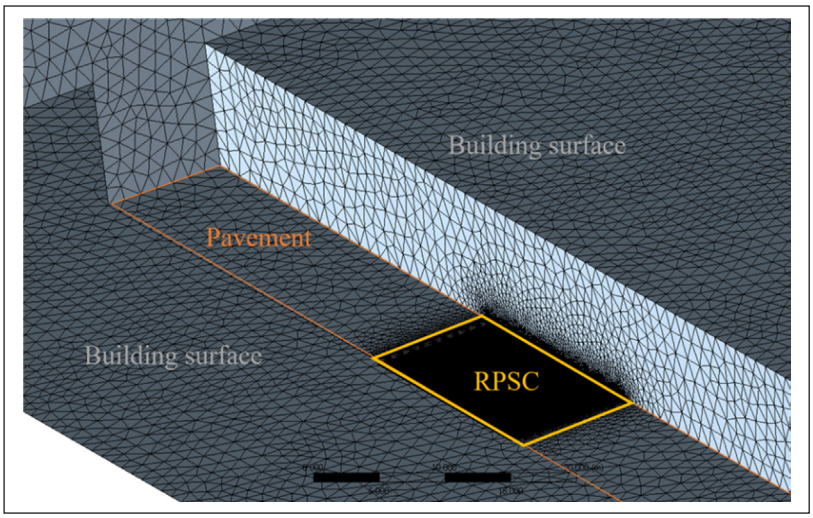

Figure 4: Mesh of the PSC domain (Fine) – bottom view.

Table 2: Material properties.

	Material	Density (kg/m³)	Specific heat, c_p (J/kgK)	Thermal conductivity (W/mK)
Pipes	Copper	8978	381	387.6
Pavement	Asphalt	230	920	1.73
Building walls	Brick	1000	1000	0.15

Water at a lower temperature was circulated through the copper pipes and brought away the pavement slab's heat. According to (Weather and Climate), the annual water temperature range is between 287K and 299K in Italy. Therefore, the initial inlet water temperature was set to 293K (19.85°C) (Bobes-Jesus et al., 2013). Copper was used as the pipe material. The top slab of the pavement was made of asphalt. The surface properties for pipes and asphalt pavement are shown in **Table 2**.

Asphalt pavement can be heated up after absorbing a large amount of solar radiation, the sun position and air temperature are changing with time. So eight different times of 26th June 2016 in Milan, Italy were selected for analysing the PSC system performance under different environmental conditions. The water velocity was 0.25 m/s with a temperature of 293K.

2.4 CFD Theory

The energy model was set to investigate the temperatures and wind flow pattern, and the viscous model was set to k-epsilon (2 equations). The steady RANS equations simulated urban turbulent airflow with the standard k-ε model based on the principle of heat conversion, continuity and momentum. In this model, the transport equation for turbulence kinetic energy (k) and dissipation rate (ε) allows the airflow to be fully turbulent solved (Fluent, 2011). Discrete ordinate (DO) and solar ray tracing were used as the radiation model for evaluating the impact of solar radiation on the surface temperature and PSC system performance. The governing equations can be written as follows:

Momentum equation:

$$\overline{u_j}\frac{\partial \overline{u_i}}{\partial x_j} = -\frac{1}{\rho}\frac{\partial p}{\partial x_i} + \frac{\mu}{\rho}\frac{\partial^2 \overline{u_i}}{\partial x_i \partial x_j} - \frac{\partial}{\partial x_j}\left(\overline{u_i' u_j'}\right) + f_i \quad (1)$$

Continuity equation:

$$\frac{\partial \overline{u_i}}{\partial x_i} = 0 \quad (2)$$

Heat conservation equation:

$$\overline{u_i}\frac{\partial \overline{T}}{\partial x_i} + \frac{\partial}{\partial x_i}\left(K_T \frac{\partial \overline{T}}{\partial x_i}\right) = 0 \quad (3)$$

Where $\overline{u_i}$ represent the mean speed of the airflow; ρ is the air density; μ the dynamic viscosity of the fluid; $\overline{u_i'}\,\overline{u_j'}$ is the Reynolds stress; f_i is the thermal-induced buoyant force; $\overline{T}$ is the potential temperature; K_t is the heat diffusivity

Transport equations:

$$\frac{\partial}{\partial t}(\rho k)+\frac{\partial}{\partial x_i}(\rho k u_i)=\frac{\partial}{\partial x_j}\left[\left(\mu+\frac{\mu_t}{\sigma_k}\right)\frac{\partial k}{\partial x_j}\right]+G_k+G_b-\rho\varepsilon \quad (4)$$

$$\frac{\partial}{\partial t}(\rho\varepsilon)+\frac{\partial}{\partial x_i}(\rho\varepsilon u_i)=\frac{\partial}{\partial x_j}\left[\left(\mu+\frac{\mu_t}{\sigma_\varepsilon}\right)\frac{\partial\varepsilon}{\partial x_j}\right]+C_{1\varepsilon}\frac{\varepsilon}{k}(G_k+C_{3\varepsilon}G_b)-C_{2\varepsilon}\rho\frac{\varepsilon^2}{k} \quad (5)$$

Where k is the turbulence kinetic energy; ε the rate of dissipation; G_K is the generation of turbulence kinetic energy due to changes in velocity; G_b is the generation of turbulence kinetic energy due to the buoyancy force; $C_{1\varepsilon}$, $C_{2\varepsilon}$ and $C_{3\varepsilon}$ are constant; σ_K and σ_ε represent the turbulent Prandtl numbers for k and ε respectively. The discrete ordinate (DO) model solves the radiate transfer equation (6) for a finite number of discrete solid angles each associated with a vector direction $\vec{s}$ fixed in the global Cartesian system (x, y, z) (Fluent, 2011). Hence,

$$\frac{dI(\vec{r},\vec{s})}{ds}+(a+\sigma_s)I(\vec{r},\vec{s})=an^2\frac{\sigma T^4}{\pi}+\frac{\sigma_s}{4\pi}\int_0^{4\pi}I(\vec{r},\vec{s}_t)\Phi(\vec{s}\cdot\vec{s}_t)d\Omega' \quad (6)$$

Where $\vec{r}$ is the position vector; $\vec{s}$ is the direction vector; $\vec{s}_t$ is the scattering direction vector; s is the path length; a is the absorption coefficient; n is the refractive index; σ_s is the scattering coefficient; σ is the Stefan-Boltzmann constant (5.669×10^{-8} W/m^2K^4); T is the local temperature; Φ is the phase function; Ω' represents the solid angle and I is the radiation intensity which depends on the position of the $\vec{r}$ and $\vec{s}$ vectors.

2.5 Numerical model validation

For the validation of the PSC numerical model, a laboratory experiment was conducted in the Energy Technologies Building, University of Nottingham, UK. A 600 mm length × 400 mm width × 130 mm depth PSC asphalt slab specimen sealed within an insulated box (**Figure 4**) was made of Bitumen Macadam with the properties of ρ = 2300 kg/m^3, c_p = 920 J/kgK and k = 1.73 W/mK. A 6.1 m length copper pipe with a diameter, Ø of 8 mm, with a thickness of 1 mm and with a thermal conductivity value, k_c of 413 W/mK was embedded at the slab specimen. The pipe was bent to replicate a serpentine U-PSC pipe with one water inlet nearby the side wall named Side A and one water outlet nearby the adjacent side wall, named Side B (**Figure 6 (a)**). The distance between each pass was maintained at 60 mm (**Figure 5**). The controlled water flow is expected to reduce the slab and surface temperature by extracting heat from the pavement. For heating up the asphalt specimen, 2 halogen lamps of 400W each were used with beam angle, φ of 60° from Side A and the lamp is 160 mm away from the specimen topmost surface.

The temperature at both Side A and Side B of the specimen surface, top layer, middle layer and bottom layer was measured using K-type thermocouples, see **Figure 6**. Calibration test of the thermocouples and water leakage test of the asphalt specimen was initially conducted before the specimen temperature was measured. The data was transferred and uploaded in PicoLog 6, a PC

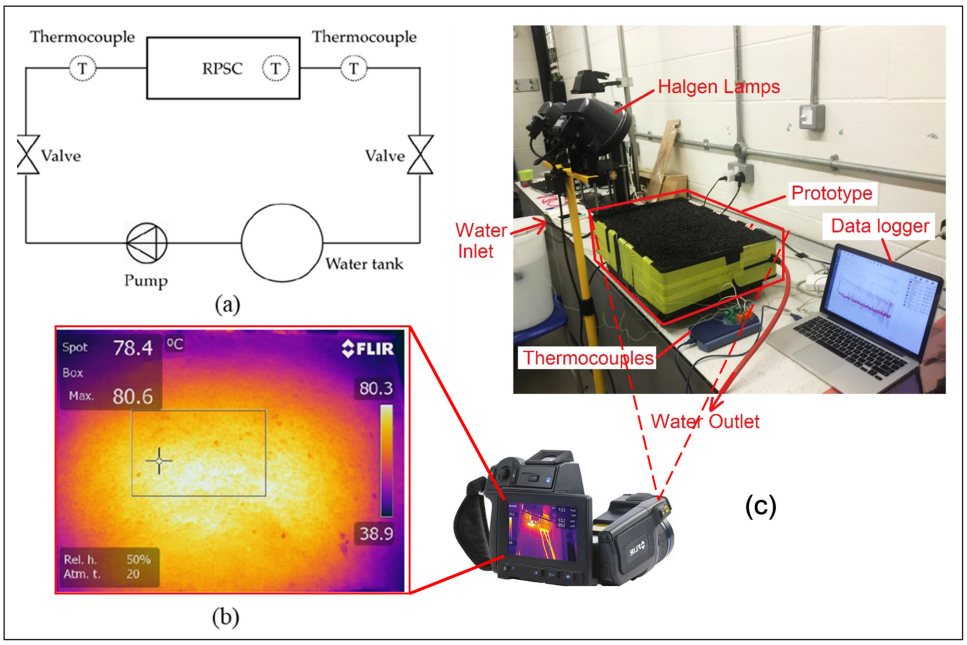

Figure 5: Laboratory experiment setup demonstrating **(a)** PSC system circulating water across heated pavement **(b)** initial surface temperature of asphalt specimen **(c)** full setup.

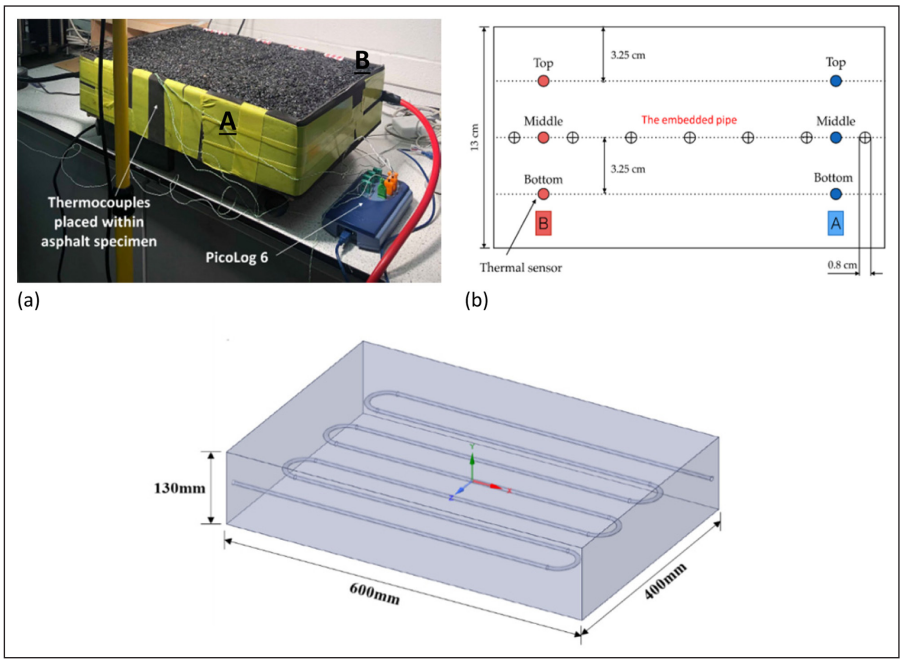

Figure 6: Temperature measurement setup showing **(a)** thermocouples placed at Side A and Side B connected to a data logger **(b)** diagram of thermocouples placed at the top, middle and bottom layer of the asphalt specimen.

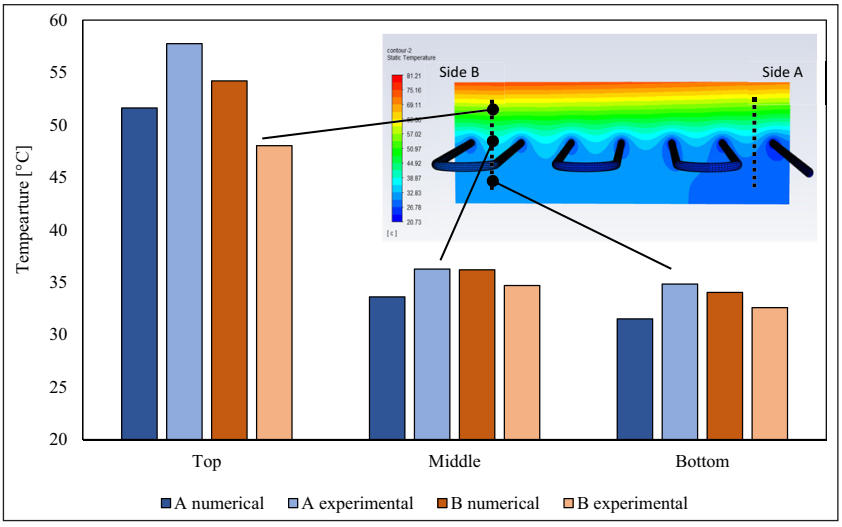

Figure 7: Validation of the numerical model of the pavement solar collector.

software which recorded the measurement at the specified locations.

The surface was heated up to 80.5°C and a total of 2 hours and 10 minutes was required to heat the asphalt specimen. The data logger began to record the temperature value at each thermocouple during the heating of the slab. After the temperature reached 80.5°C, water with ambient temperature 20–22°C began to flow into the serpentine pipe by using a pump with 240 litres/h maximum flow rate, 8.4W power, 12V DC voltage and 3 m maximum head. The water flow continued within 1-hour duration before the pump was switched off. Using FLIRthermal infrared camera, the topmost asphalt specimen surface temperature was taken every 2 minutes during the specified duration. The validation of the urban canyon modelling was carried out and fully detailed in previous works (Nasir et al., 2015).

3. Results and Discussion

3.1 Experimental validation for software modelling

The temperature field was validated by comparing the obtained temperature from the simulation with the temperature based on the experimental results. The comparison was carried out by measuring a similar location where the thermocouples were placed in the PSC prototype, see the validation results in **Figure 7**. The temperature results at three positions according to the asphalt depth (top, middle and bottom of side A and side B) between experiment and simulation were compared. Based on **Figure 7**, the simulation results were underestimated up to 5°C at the top position; however, the variance became nominal at the middle and bottom positions, by 1–3°C. Overall, the temperature distribution profile across the pavement depth of the simulation was compatible with the temperature profile across the pavement depth of the experiment. It implies from the

validation that the temperature field of the constructed model in this study can be used for further analysis.

3.2 Effect of mesh sizing on results accuracy

Mesh size is one factor that influences the simulation result; **Figure 8** shows the temperature difference among three different mesh sizes. The result for pipe 1, pipe 5 and 6 were almost the same; the maximum temperature difference was between pipe 4 and pipe 8, which was 0.21°C. The outlet water temperatures were in the range of 20.94°C to 22.01°C, which means the temperature differences among these 9 pipes were up to 1.07°C. Therefore, the percentage difference (19.53%) was not negligible. In order to obtain high accuracy results, the Fine mesh size was selected for future simulation and analysis.

3.3 Effect of the PSC system on urban canyon temperature

Figure 9 (a) shows the temperature distribution of the urban canyon ground and building surfaces. Due to the shadowing effect caused by the windward building, the lower surface temperature was (45–50°C) was observed near the windward building. It can also be observed that the pavement had about 10°C higher temperature than the building sidewalls and air. It can be clearly observed that the PSC system reduced the temperature of the pavement surface in the middle of the canyon (20% of the canyon). The temperature of the urban street canyon cross-section is shown in **Figure 9 (b)**. Section 1 is the area above the pipe-embedded-pavement and section 2 is the area without the PSC system. The near-ground-air in section 2 had about 10°C higher than that of section 1, which means the PSC system could reduce air temperature. It also shows that the air near the building surface had a higher temperature than the air because of solar radiation. When the PSC cooled down the pavement temperature and air temperature, there would be less convective heat transfer between walls and air because of the smaller temperature differences. In this way, the building cooling energy demand would decrease. The detailed analytical results of the PSC's temperatures and performance are presented in the following five sub-sections.

The most notable differences after adding the PSC system are the pavement surface temperature, and adjacent wall temperature of Building A. **Figure 10** shows the pipe-embedded-pavement section's temperature was about 28% lower than the areas without pipes. According to the figure, without the PSC system, the temperature of the unshaded pavement area was heated up to about 65°C, the maximum value can reach 71°C. With the PSC system, the temperature was about 47°C to 67°C. Although the temperature reduction was not significant in the shadowed area, the minimum pavement temperature dropped to about 28°C, which is even lower than the ambient air temperature (29.85°C). The pavement surface temperature was not uniform in the pipe-embedded area; it shows that the temperature distribution had the same pattern as the pipe locations and hence in further studies, we will attempt to improve the temperature distribution.

For the simulated period, four pipes were located in the shaded area or near Building B. Due to the shadowing effect, the pavement surface close to Building A had a higher temperature (60°C to 70°C) than the surface close

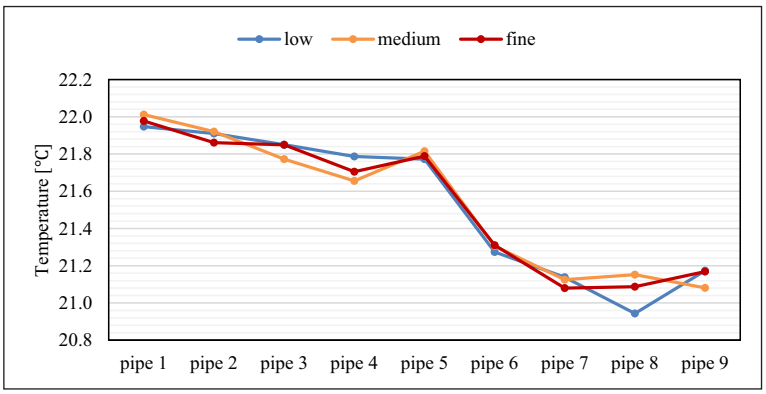

Figure 8: Grid sensitivity analysis.

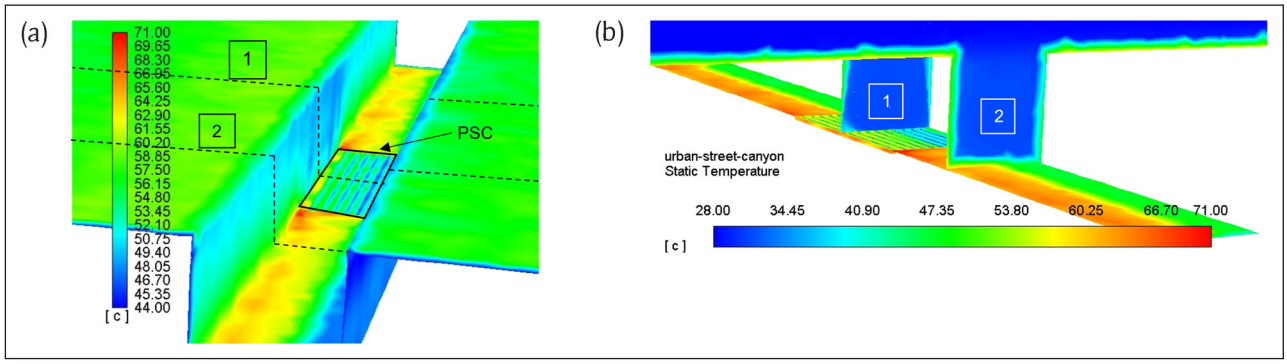

Figure 9: (a) Surface temperature contour of the street canyon and surrounding buildings and **(b)** cut section temperature contour of the urban street canyon.

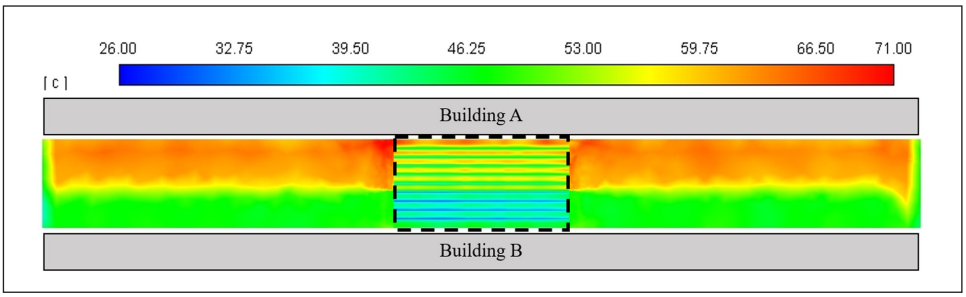

Figure 10: Temperature contour of pavement with PSC with inlet water velocity of 0.25 m/s.

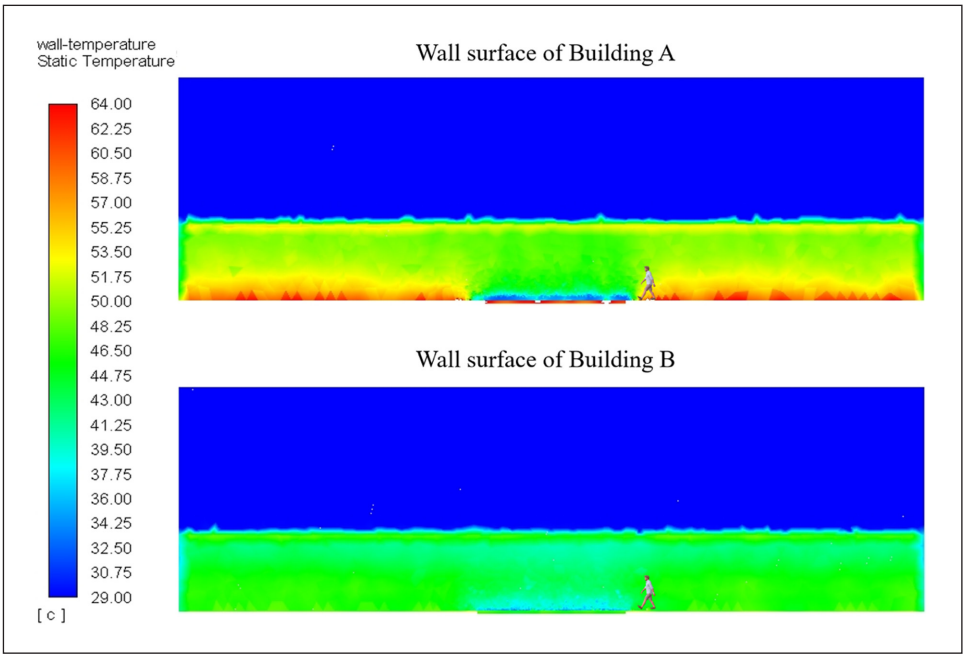

Figure 11: Wall temperatures of Building A and Building B.

to Building B (about 47°C). The building obstructed some solar radiation because Building B was located south of the pavement. The shadow effect prevented the pavement from being heated at a higher temperature; **Figure 10** illustrated that the temperature difference between shaded and unshaded area was about 15°C. The central pavement area embedded with the cooling pipes had a much lower surface temperature in both shaded and unshaded areas; the cooling effect was more significant especially in the unshaded area, the temperature was reduced up to 20°C. The ambient air would have a lower temperature when it was close to the cool surfaces, improving the thermal environment for pedestrians in summer. As building energy demand is related to the ambient temperature, the cool pavement could reduce the cooling energy demand. Another advantage of cooling the surface is reducing the high-temperature damage to car tyres. It is stated by (DKT, 2020) that the higher temperature will increase the tyre pressure, which may cause the tyres to blow out. The tyre pressure drops by approximately 0.19 pounds per square inch (psi) for every decrease of 1°C. The result indicates that the PSC system can reduce the surface temperature, particularly the areas with very high temperature and exposed road surfaces. It also shows the importance of carrying out a detailed analysis which will help position the PSC system and maximise its performance.

3.4 Effect of the PSC system on building and air temperature

The previous section shows that when pipes were embedded under the road, the pavement surface temperature was much lower than that without the pipes. As the air temperature was always lower than the pavement surface temperature, the direction of convection heat transfer should always come from the pavement to the air. It can be indicated that there would be less heat transfer between air and pavement surface, because of smaller surface temperature difference. Therefore, low pavement surface temperature can decrease the surrounding air temperature and would be necessary to minimise the UHI effect.

Figure 11 shows the wall temperature contours of building surfaces, the wall section, which was close to the pipe area had much lower temperature than other sections. The wall surface of Building A shows clearly that the temperature reduction was significant in lower height areas. With the PSC system, the unshaded wall surface temperature ranged between 44°C to 48°C. At the pedestrian level, the wall surface temperature reduction was up to 10°C.

It can be observed that the PSC system had a more significant influence on the temperature of wall surfaces which were closer to the ground. From the figure of Building A, it shows the PSC system can reduce the

near-ground-wall temperature about 10°C to 15°C. **Figure 12** shows horizontal cross-section contours of the air temperatures at different heights (0.1 m, 0.5 m, 1.0 m, 1.5 m and 2.0 m). Without the PSC system, the overall air temperature decreased with the height increasing, which indicates that high-temperature pavement mainly affected the air temperature at a low height.

As observed in **Figure 12**, the air temperature near the ground surface (0.1 m) can be as high as 67°C and reduces with the height. The cooling effect provided by the PSC system was significant at the lower height areas; the air temperature can be cooled down up to about 30°C. The building wall surfaces had a higher temperature because of direct solar radiation and indirect radiation, so the walls emitted heat to the surrounding air and increased the air temperature up to 51°C. According to the temperature contours at five heights, it can be predicted that at the height of 2.0 m and above, the PSC system's influence was minimal. For the spaces which were lower than 1.5 m, the air above the pipe-embedded-pavement section had a lower temperature than other areas; the temperature reduction was about 5°C to 10°C. Human average height is lower than 2.0 m so that the PSC system can provide a more comfortable thermal environment for pedestrians.

Six points were selected to investigate the relationship among the air temperature, location and height for the positions point a, b, c, d, e and f as shown in **Figure 13** (a) and the air temperatures profiles from 0.0 m to 2.0 m height were plotted in **Figure 13 (b)**. For this analysis, the case of the inlet water velocity of 0.25 m/s was chosen, and the pavement material was asphalt.

The six points were selected symmetrically, point a, c and e were close to the unshaded wall, and point b, d and f

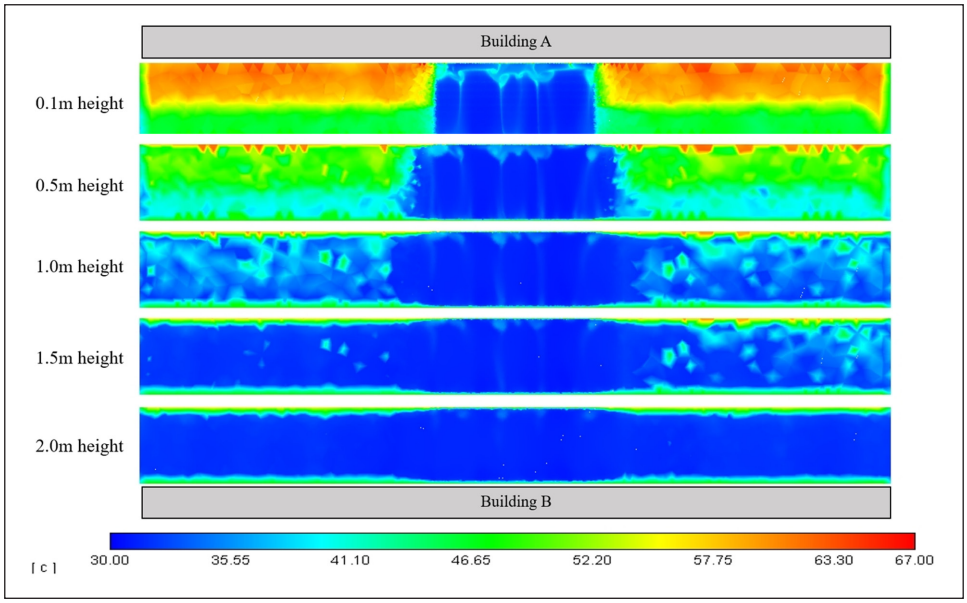

Figure 12: Air temperature distributions in different heights: horizontal cross-section contours from 0.1 m to 2 m.

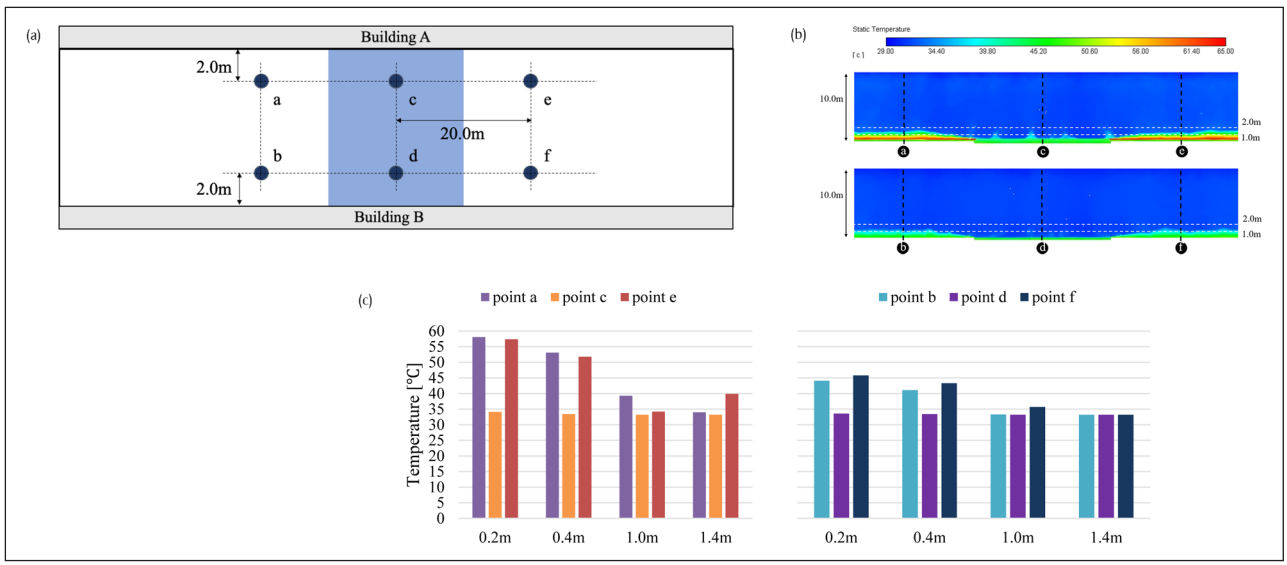

Figure 13: (a) Selected point locations (not to scale), **(b)** temperature profile at the six locations (inlet water velocity 0.25 m/s with a temperature of 19.85°C, wind speed 2 m/s with a temperature of 29.85°C) and **(c)** air temperatures of the six points at different heights.

were close to the shaded wall. Compared to point a, c and e, point b, d and f had much lower air temperature, which was as same as discussed in section 4.1. At the height of 0.4 m, the temperature difference was 11°C, and at the height of 0.8 m, the temperature difference was 9°C, the air temperature difference between shaded and unshaded area.

Below the height of 0.88 m, the air temperatures at point c and d were much lower than those at point a, b, e and f. The gradients show that the temperature decreased much faster at point c and d than other points. The figure shows the cooling effect by the PSC system was notable at the low height spaces. In the unshaded area, with the PSC system, the air temperature can decrease up to 33.9°C at a height of 0.2 m. However, at this height without the PSC system, the air temperature was up to 57.5°C. Although below the 0.9 m height, air temperatures in the shaded area were lower than the unshaded area, they were even higher than that at point c, which is the unshaded area above pipe-embedded-pavement. Data collected from the six points confirmed that the PSC system significantly impacted the street canyon thermal environment and could reduce the air temperature near the pavement surface. It can cool down the air temperature at the pedestrian level effectively.

3.5 Effect of varying air temperature and solar radiation on pipe outlet water temperature/potential thermal energy collection

According to the above analysis, the pipes under shaded area dissipated less heat from the pavement than the pipes located in the unshaded area. The selected date for this work was 26th June 2016 (Timeanddate.com). In this section, assuming that the initial inlet water temperature (19.85°C), inlet water velocity (0.25 m/s) and wind speed (2 m/s) were the same. **Table 3** shows the ambient air temperature at different time of the day; the air temperatures are always higher than the circulating water temperature.

Building A is located in the north of the urban street canyon, and Building B is located in the south. The shadow area on the pavement changes with the sun position changing. The sun was in the north of the urban street canyon in the morning, as shown in **Figure 14**, the shadow is caused by Building A before 12 am. The figure clearly showed that in the unshaded area, the pavement temperature is related to the air temperature. When the ait temperature is higher, the pavement surface would have a higher temperature. It shows a significant difference between the pavement surface temperatures of 2 pm and 6 pm. Although the air temperatures were the same at 2 pm and 6 pm, the shaded area at 6 pm had much lower surface temperature than at 2 pm. Therefore, both air temperature and solar radiation patterns can influence the pavement surface temperature. The CFD results showed that at all selected times, the pipe-embedded areas have lower temperatures. The PSC system can provide cooling effect at all selected times, which means when there is no direct solar radiation coming to the surface, the cold water pipes could still reduce the pavement surface temperature.

The outlet water temperatures of the nine pipes are plotted in **Figure 15**, which are used to show the cooling

Table 3: Air temperature at different times in the case study location (Timeanddate.com).

Time	8am	10am	11am	12am	1pm	2pm	4pm	6pm
Temperature [°C]	22	25	26	27	28	30	31	30

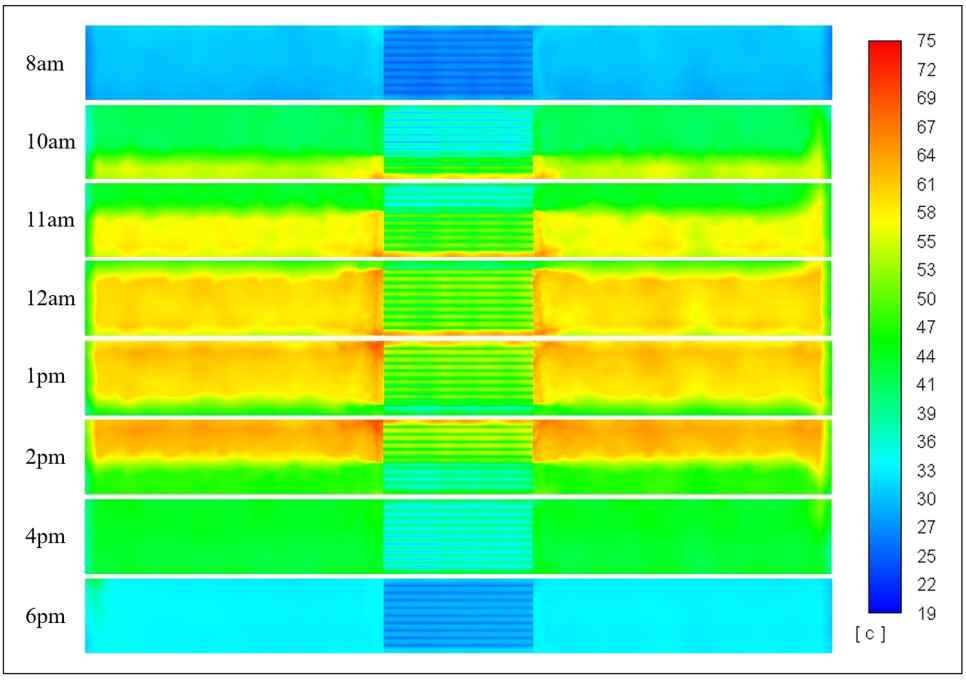

Figure 14: Pavement surface temperature contours at different times.

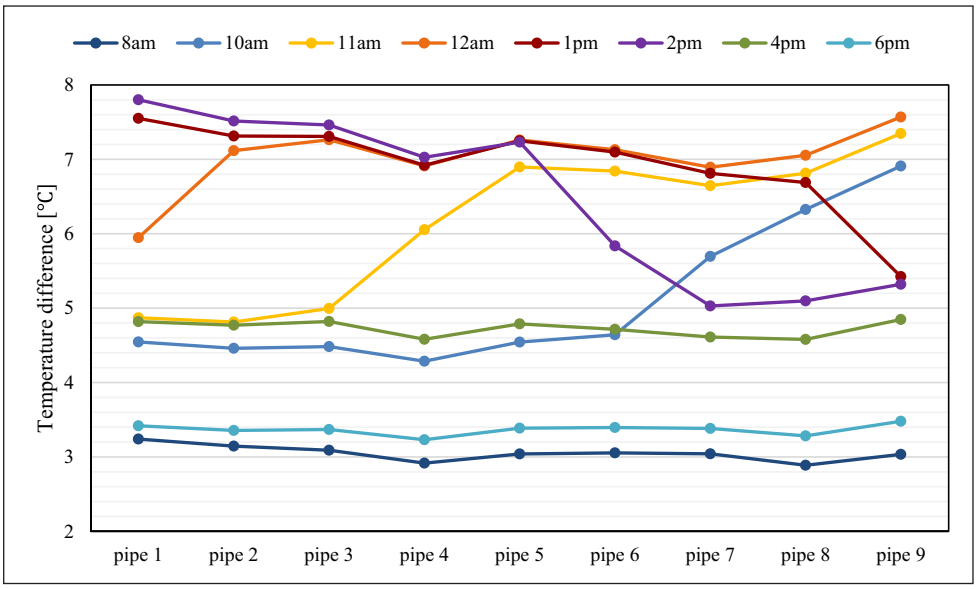

Figure 15: Temperature difference between outlet and inlet water – at different times of the day.

effect provided by the PSC system. It showed that at noon the PSC system has a better cooling effect. The PSC system at 8 am and 6 pm showed low cooling effect than other times. There was no direct solar radiation to the pavement surface at 8 am, 4 pm and 6 pm, the asphalt surface cannot absorb a large amount of heat, the pavement was not heated up to a high temperature. Therefore, although the air temperature was high at 6 pm, the outlet water temperature can only increase by about 3.4°C in the late afternoon. In the morning, the air temperature was low, and there was no direct solar radiation, so the increment of outlet water temperature was also not significant.

When there was direct solar radiation coming to the pavement, the outlet water temperatures were much higher than the inlet temperatures. At 12 am, the water temperature average increment of the nine pipes was 7.02°C, while at 8am the average increment was 3.05°C. At 2 pm, the temperature maximum of increment was 7.8°C. For the pipes in the unshaded area, the inlet and outlet temperature differences are about 7°C, which means the circulating water temperature increased by 35%. The results showed that it is necessary to consider the PSC system operating time to obtain higher efficiency.

4. Conclusion

This research investigated the impact of the PSC system on the urban street canyon thermal environment, including building surface temperatures, pavement temperature and cooling effect provided by water pipes. A coupled approach was developed to combine both the urban street canyon domain and the PSC domain, which allows analysing the impact of PSC on the urban street canyon temperature directly. The numerical modelling of the PSC was validated against experimental data and showed good agreement. Analysis of the PSC system was performed for a section of the whole urban canyon pavement.

Based on the set conditions, the results showed that unshaded pavement's surface temperature could be reduced up to about 10°C in the unshaded area with the PSC system embedded under the road. Shadows caused by the building reduced the pavement surface temperature to about 15°C. In the shaded area, the surface temperature reduction was smaller than in the unshaded area; it provided up to 7°C temperature reduction of the pavement surface based on the simulated conditions.

Meanwhile, the PSC system also significantly reduced the wall surface temperatures, especially in the areas that are closed to the pavement. By comparing the air temperature distribution contours of 0.1 m, 0.5 m, 1.0 m, 1.5 m and 2.0 m height, it was found that the air temperature can be cooled down to about 30°C at low height area by the PSC system. The region's air temperature above the pipe-embedded-pavement area had a lower temperature than other areas at the height below 1.5 m; temperature reduction was up to 5°C–10°C based on the simulated conditions. The analysis of the temperature profiles at six different locations confirmed that the PSC system could reduce the air temperature. Air temperature can be reduced up to 34°C at a height of 0.2 m. Therefore, the PSC system could provide a better thermal environment for pedestrians.

Finally, analysed the impact of the solar condition and air temperature on the PSC system performance. Eight different times of one day were selected for this section. The results showed that with higher air temperature and direct solar radiation, the PSC system could provide more cooling effect. In the early morning, the water temperature increment was 15.2% and at noon can be 35.1%. When the system operating under the condition which had the same air temperature but different time, the solar condition also can bring 15.5% difference (water temperature increment was 32.4% at 4 pm but was 16.9% at 6 pm). It is necessary to consider the environmental conditions for higher operating performance efficiency.

According to the analysis, the main benefit of the PSC system is to reduce building cooling energy demand and improve a comfortable thermal environment for pedestrians, as well as protecting the car tyres during hot days.

5. Future works

According to the above analysis, both pipe location and inlet water velocity impacted the PSC system performance; it also highlighted the building wall surface temperatures were affected by the pavement and surrounding air temperature. The pipe-embedded-pavement section in this research was only 20% of the total pavement area; in our future work, the full-size PSC system will be simulated in a larger scale urban canyon model. The building wall temperatures should be analysed using more realistic building models to show the influence on building cooling energy demand. Initial cost, operation and maintenance costs should also be considered in order to improve system efficiency and provide a better cooling effect for the surrounding environment. Other parameters such as pipe position, pipe depth and working system period need to be discussed depending on the local environment. Therefore, actual climate conditions should be carried out in order to improve result quality (Santamouris, 2020), and future research should be extended to the whole year for accurate predictions.

6. Nomenclature

CFD	Computational Fluid Dynamics
DO	Discrete Ordinate
PSC	Pavement Solar Collector
SVF	Sky View Factor
UHI	Urban Heat Island
a	Absorption coefficient
$C_{1\varepsilon}$	Constant
$C_{2\varepsilon}$	Constant
$C_{3\varepsilon}$	Constant
C_p	Specific heat capacity
f_i	Thermal-induced buoyant force
G_b	generation of turbulence kinetic energy due to the buoyancy force
G_k	generation of turbulence kinetic energy due to changes in velocity
I	Radiation intensity
k	Turbulence kinetic energy
K_T	Heat diffusivity
n	Refractive index
$\vec{r}$	Position vector
T	local temperature
s	Path length
$\vec{s}$	Direction vector
$\vec{s}_t$	Scattering direction vector
$\overline{T}$	Potential temperature
$\overline{u_i}$	Mean speed of the airflow
$\overline{u_i'}\,\overline{u_j'}$	Reynolds stress
ε	Rate of dissipation
ρ	Air density
μ	Fluid dynamic viscosity
σ	Stefan-Boltzmann constant
σ_ε	Turbulent Prandtl numbers for ε
σ_k	Turbulent Prandtl numbers for k
σ_s	Scattering coefficient
Φ	Phase function
Ω'	Solid angle
$\emptyset$	Pipe diameter
φ	Beam angle

Acknowledgements

The authors would like to thank the support of the Department of Architecture and Built Environment of the University of Nottingham for providing the facility for carrying out the simulations and experiments.

Competing Interests

The authors have no competing interests to declare.

References

Ai, ZT and **Mak, CM.** 2015. From street canyon microclimate to indoor environmental quality in naturally ventilated urban buildings: Issues and possibilities for improvement. *Building and Environment*, 94: 489–503. DOI: https://doi.org/10.1016/j.buildenv.2015.10.008

Ai, ZT and **Mak, CM.** 2017. CFD simulation of flow in a long street canyon under a perpendicular wind direction: Evaluation of three computational settings. *Building and Environment*, 114: 293–306. DOI: https://doi.org/10.1016/j.buildenv.2016.12.032

Berdahl, P and **Bretz, SE.** 1997. Preliminary survey of the solar reflectance of cool roofing materials. *Energy and Building*, 25: 149–158. DOI: https://doi.org/10.1016/S0378-7788(96)01004-3

Bobes-Jesus, V, Pascual-Muñoz, P, Castro-Fresno, D and **Rodriguez-Hernandez, J.** 2013. Asphalt solar collectors: A literature review. *Applied Energy*, 102: 962–970. DOI: https://doi.org/10.1016/j.apenergy.2012.08.050

Bouyer, J, Inard, C and **Musy, M.** 2011. Microclimatic coupling as a solution to improve building energy simulation in an urban context. *Energy and Buildings*, 43: 1549–1559. DOI: https://doi.org/10.1016/j.enbuild.2011.02.010

Chen, BL, Bhowmick, S and **Mallick, RB.** 2009. Harvesting energy from asphalt pavements and reducing the heat island effect. *International Journal of Sustainable Engineering*, 2: 214–228. DOI: https://doi.org/10.1080/19397030903121950

Chiarelli, A, Al-Mohammedawi, A, Dawson, AR and **García, A.** 2017. Construction and configuration of convection-powered asphalt solar collectors for the reduction of urban temperatures. *International Journal of Thermal Sciences*, 112: 242–251. DOI: https://doi.org/10.1016/j.ijthermalsci.2016.10.012

Ciobanu, D, Eftimie, E and **Jaliu, C.** 2014. The Influence of Measured/simulated Weather Data on Evaluating the Energy Need in Buildings. *Energy Procedia*, 48: 796–805. DOI: https://doi.org/10.1016/j.egypro.2014.02.092

Weather-and-climate. Available: https://weather-and-climate.com/average-monthly-water-Temperature, gallipoli,Italy [Accessed October 2019].

Daniels, JW, Heymsfield, E and **Kuss, M.** 2019. Hydronic heated pavement system performance using a solar water heating system with heat pipe evacuated tube solar collectors. *Solar Energy*, 179: 343–351. DOI: https://doi.org/10.1016/j.solener.2019.01.006

DKT. 2020. *How the temperature and weather affects tyre pressures* [Online]. [Accessed March 2020].

Evola, AG, Fichera, A, Martinico, F, Nocera, F and **Pagano, A.** 2017. UHI effects and strategies to improve outdoor thermal comfort in dense and old neighbourhoods. DOI: https://doi.org/10.1016/j.egypro.2017.09.589

Fluent, A. 2011. User's Guide.

Gaitani, N, Mihalakakou, G and **Santamouris, M.** 2007. On the use of bioclimatic architecture principles in order to improve thermal comfort conditions in outdoor spaces. *Building and Environment*, 42: 317–324. DOI: https://doi.org/10.1016/j.buildenv.2005.08.018

Guattari, C, Evangelisti, L and **Balaras, CA.** 2018. On the assessment of urban heat island phenomenon and its effects on building energy performance: A case study of Rome (Italy). *Energy and Buildings*, 158: 605–615. DOI: https://doi.org/10.1016/j.enbuild.2017.10.050

Guldentops, G, Nejad, AM, Vuye, C, Van Den Bergh, W and **Rahbar, N.** 2016. Performance of a pavement solar energy collector: Model development and validation. *Applied Energy*, 163: 180–189. DOI: https://doi.org/10.1016/j.apenergy.2015.11.010

Akbari, H, Pomerantz, M and **Taha, H.** 2001. Cool surfaces and shade trees to reduce energy use and improve air quality in urban areas. *Solar Energy*, 70: 295–310. DOI: https://doi.org/10.1016/S0038-092X(00)00089-X

Hasebe, M, Kamikawa, Y and **Meiarashi, S.** 2016. Thermoelectric generators using solar thermal energy in heated road pavement. *Thermoelectrics*.

Karasawa, TN and **Ezumi, KK.** 2006. Evaluation of performance of water-retentive concrete block pavements. *8th International conference on concrete block paving*.

Lin, Y, Ichinose, T, Yamao, Y and **Mouri, H.** 2020. Wind velocity and temperature fields under different surface heating conditions in a street canyon in wind tunnel experiments. *Building and Environment*, 168. DOI: https://doi.org/10.1016/j.buildenv.2019.106500

Ma, X, Fukuda, H, Zhou, D and **Wang, M.** 2019. Study on outdoor thermal comfort of the commercial pedestrian block in hot-summer and cold-winter region of southern China-a case study of The Taizhou Old Block. *Tourism Management*, 75: 186–205. DOI: https://doi.org/10.1016/j.tourman.2019.05.005

Mallick, RB, Chen, BL and **Bhowmick, S.** 2009. Reduction of urban heat effect through harvest of heat energy from asphalt pavements. *Proceedings on the heat island conference*. DOI: https://doi.org/10.1080/19397030903121950

Memon, RA, Leung, DYC and **Liu, C-H.** 2010. Effects of building aspect ratio and wind speed on air temperatures in urban-like street canyons. *Building and Environment*, 45: 176–188. DOI: https://doi.org/10.1016/j.buildenv.2009.05.015

Murphy, M. 2011. Design and Construction of Roads and Accesses to Adoptable Standards, Developer Guidance.

Nasir, DSNM, Hughes, BR and **Calautit, JK.** 2015. A study of the impact of building geometry on the thermal performance of road pavement solar collectors. *Energy*, 93: 2614–2630. DOI: https://doi.org/10.1016/j.energy.2015.09.128

Nasir, DSNM, Hughes, BR and **Calautit, JK.** 2017a. A CFD analysis of several design parameters of a road pavement solar collector (RPSC) for urban application. *Applied Energy*, 186: 436–449. DOI: https://doi.org/10.1016/j.apenergy.2016.04.002

Nasir, DSNM, Hughes, BR and **Calautit, JK.** 2017b. Influence of urban form on the performance of road pavement solar collector system: Symmetrical and asymmetrical heights. *Energy Conversion and Management*, 149: 904–917. DOI: https://doi.org/10.1016/j.enconman.2017.03.081

Nasir, DSNM, Hughes, BR, Calautit, JK, Aquino, AI and **Shahzad, S.** 2017c. Effect of Urban Street Canyon Aspect Ratio on Thermal Performance of Road Pavement Solar Collectors (RPSC). *Energy Procedia*, 105: 4414–4419. DOI: https://doi.org/10.1016/j.egypro.2017.03.936

Nunez, M and **Oke, TR.** 1976. The Energy Balance of an Urban Canyon. *Journal of Applied Meteorology*, 16: 11–19. DOI: https://doi.org/10.1175/1520-0450(1977)016<0011:TEBOAU>2.0.CO;2

Oke, TR. 1987. *Boundary Layer Climates*. New York: Routledge.

Papadimitriou, CN, Psomopoulos, CS and **Kehagia, F.** 2019. A review on the latest trend of Solar Pavements in Urban Environment. *Energy Procedia*, 157: 945–952. DOI: https://doi.org/10.1016/j.egypro.2018.11.261

Pascual-Muñoz, P, Castro-Fresno, D, Serrano-Bravo, P and **Alonso-Estébanez, A.** 2013. Thermal and hydraulic analysis of multilayered asphalt pavements as active solar collectors. *Applied Energy*,

111: 324–332. DOI: https://doi.org/10.1016/j.apenergy.2013.05.013

Sailor, D. 1995. Simulated Urban Climate Response to Modifications in Surface Albedo and Vegetative Cover. *Journal of Applied Meteorology*, 34: 1694–1700. DOI: https://doi.org/10.1175/1520-0450-34.7.1694

Santamouris, M. 2013. Using cool pavements as a mitigation strategy to fight urban heat island—A review of the actual developments. *Renewable and Sustainable Energy Reviews*, 26: 224–240. DOI: https://doi.org/10.1016/j.rser.2013.05.047

Santamouris, M. 2020. Recent progress on urban overheating and heat island research. Integrated assessment of the energy, environmental, vulnerability and health impact. Synergies with the global climate change. *Energy and Buildings*, 207. DOI: https://doi.org/10.1016/j.enbuild.2019.109482

Santamouris, M, Cartalis, C, Synnefa, A and **Kolokotsa, D.** 2015. On the impact of urban heat island and global warming on the power demand and electricity consumption of buildings—A review. *Energy and Buildings*, 98: 119–124. DOI: https://doi.org/10.1016/j.enbuild.2014.09.052

Sketchfab. 2020. Available: https://sketchfab.com/3d-models/male-3-walking-d08b5f1d023c48acadbca4d40ebfd848 [Accessed March 2020].

Sun, Y and **Augenbroe, G.** 2014. Urban heat island effect on energy application studies of office buildings. *Energy and Buildings*, 77: 171–179. DOI: https://doi.org/10.1016/j.enbuild.2014.03.055

Timeanddate.com. *Past weather in Milan Italy* [Online]. Available: https://www.timeanddate.com/weather/italy/milan/historic?month=6&year=2016 [Accessed].

Wang, KW and **Vineyard, EA.** 2011. Adsorption refrigeration. *ASHRAE*, 14.

Yang, J, Wang, Z-H, Kaloush, KE and **Dylla, H.** 2016. Effect of pavement thermal properties on mitigating urban heat islands: A multi-scale modeling case study in Phoenix. *Building and Environment*, 108: 110–121. DOI: https://doi.org/10.1016/j.buildenv.2016.08.021

Zhu, Y, Liu, J, Hagishima, A, Tanimoto, J, Yao, Y and **Ma, Z.** 2007. Evaluation of coupled outdoor and indoor thermal comfort environment and anthropogenic heat. *Building and Environment*, 42: 1018–1025. DOI: https://doi.org/10.1016/j.buildenv.2005.10.019

How to cite this article: Xu, W, Jimenez-Bescos, C, Pantua, CAJ, Calautit, J and Wu, Y. 2021. A Coupled Modelling Method for the Evaluation of the Impact of Pavement Solar Collector on Urban Air Temperature and Thermal Collection. *Future Cities and Environment*, 7(1): 2, 1–16. DOI: https://doi.org/10.5334/fce.109

Submitted: 23 September 2020 **Accepted:** 01 February 2021 **Published:** 19 February 2021

]u[*Future Cities and Environment*, is a peer-reviewed open access journal published by Ubiquity Press.

OPEN ACCESS